Available online at www.sciencedirect.com
SCIENCE DIRECT®
ICARUS
Icarus 166 (2003) 238–247
www.elsevier.com/locate/icarus

The variability of Mercury's exosphere by particle and radiation induced surface release processes

H. Lammer,[a,*] P. Wurz,[b] M.R. Patel,[c] R. Killen,[d] C. Kolb,[a] S. Massetti,[e] S. Orsini,[e] and A. Milillo[e]

[a] *Space Research Institute, Department of Extraterrestrial Physics, Austrian Academy of Sciences, Schmiedlstr. 6, A-8042 Graz, Austria*
[b] *Physics Institute, University of Bern, Sidlerstr. 5, CH-3012 Bern, Switzerland*
[c] *Planetary and Space Sciences Research Institute, The Open University, Walton Hall, Milton Keynes, MK7 6AA, UK*
[d] *Department for Astronomy, University of Maryland, College Park, MD 20742, USA*
[e] *Istituto di Fisica dello Spazio Interplanetario, Consiglio Nazionale delle Ricerche, via del Fosso del Cavaliere, 100, I-00133, Roma, Italy*

Received 18 November 2002; revised 18 August 2003

Abstract

Mercury's close orbit around the Sun, its weak intrinsic magnetic field and the absence of an atmosphere ($P_{\mathrm{surface}} < 1 \times 10^{-8}$ Pa) results in a strong direct exposure of the surface to energetic ions, electrons and UV radiation. Thermal processes and particle-surface-collisions dominate the surface interaction processes leading to surface chemistry and physics, including the formation of an exosphere ($N \leqslant 10^{14}$ cm^{-2}) in which gravity is the dominant force affecting the trajectories of exospheric atoms. NASA's Mariner 10 spacecraft observed the existence of H, He, and O in Mercury's exosphere. In addition, the volatile components Na, K, and Ca have been observed by ground based instrumentation in the exosphere. We study the efficiency of several particle surface release processes by calculating stopping cross-sections, sputter yields and exospheric source rates. Our study indicates surface sputter yields for Na between values of about 0.27 and 0.35 in an energy range from 500 eV up to 2 keV if Na^+ ions are the sputter agents, and about 0.037 and 0.082 at an energy range between 500 eV up to 2 keV when H^+ are the sputter agents and a surface binding energy of about 2 eV to 2.65 eV. The sputter yields for Ca are about 0.032 to 0.06 and for K atoms between 0.054 to 0.1 in the same energy range. We found a sputter yield for O atoms between 0.025 and 0.04 for a particle energy range between 500 eV up to 2 keV protons. By taking the average solar wind proton surface flux at the open magnetic field line area of about 4×10^8 cm^{-2} s^{-1} calculated by Massetti et al. (2003, Icarus, in press) the resulting average sputtering flux for O is about 0.8–1.0 $\times 10^7$ cm^{-2} s^{-1} and for Na approximately 1.3–1.6 $\times 10^5$ cm^{-2} s^{-1} depending on the assumed Na binding energies, regolith content, sputtering agents and solar activity. By using lunar regolith values for K we obtain a sputtering flux of about 1.0–1.4 $\times 10^4$ cm^{-2} s^{-1}. By taking an average open magnetic field line area of about 2.8×10^{16} cm^2 modelled by Massetti et al. (2003, Icarus, in press) we derive an average surface sputter rate for Na of about 4.2×10^{21} s^{-1} and for O of about 2.5×10^{23} s^{-1}. The particle sputter rate for K atoms is about 3.0×10^{20} s^{-1} assuming lunar regolith composition for K. The sputter rates depend on the particle content in the regolith and the open magnetic field line area on Mercury's surface. Further, the surface layer could be depleted in alkali. A UV model has been developed to yield the surface UV irradiance at any time and latitude over a Mercury year. Seasonal and diurnal variations are calculated, and Photon Stimulated Desorption (PSD) fluxes along Mercury's orbit are evaluated. A solar UV *hotspot* is created towards perihelion, with significant average PSD particle release rates and Na fluxes of about 3.0×10^6 cm^{-2} s^{-1}. The average source rates for Na particles released by PSD are about 1×10^{24} s^{-1}. By using the laboratory obtained data of Madey et al. (1998, J. Geophys. Res. 103, 5873–5887) for the calculation of the PSD flux of K atoms we get fluxes in the order of about 10^4 cm^{-2} s^{-1} along Mercury's orbit. However, these values may be to high since they are based on idealized smooth surface conditions in the laboratory and do not include the roughness and porosity of Mercury's regolith. Further, the lack of an ionosphere and Mercury's small, temporally and spatially highly variable magnetosphere can result in a large and rapid increase of exospheric particles, especially Na in Mercury's exosphere. Our study suggests that the average total source rates for the exosphere from solar particle and radiation induced surface processes during quiet solar conditions may be of the same order as particles produced by micrometeoroid vaporization. We also discuss the capability of in situ measurements of Mercury's highly variable particle environment by the proposed NPA-SERENA instrument package on board ESA's BepiColombo Mercury Planetary Orbiter (MPO).

* Corresponding author.
E-mail address: helmut.lammer@oeaw.ac.at (H. Lammer).

0019-1035/$ – see front matter © 2003 Elsevier Inc. All rights reserved.
doi:10.1016/j.icarus.2003.08.012

Keywords: Mercury; Surface; Regolith

1. Introduction

The Ultraviolet Spectrometer (UVS) on board of the Mariner 10 spacecraft observed in Mercury's exosphere H, He and O atoms (Broadfoot et al., 1976). Exospheric Na, K and Ca atoms were discovered by ground based observations (Potter and Morgan, 1985, 1986; Bida et al., 2000). Of all discovered elements only Na can be monitored over long timescales by studying its strong resonance transitions in the visible region. The observations show that the Na content is highly variable and column densities changes on timescales less than a day with common high latitude enhancements, which have been related to solar wind magnetosphere interaction or variations in the regolith composition (e.g., Potter and Morgan 1990, 1997; Killen et al., 1990, 1999, 2001, 2003; Sprague et al., 1997, 1998; Potter et al., 1999; Stern et al., 2000).

The trapping and circulation of solar wind particles inside a planetary magnetosphere, or the precipitation of local picked up ion plasma onto a planetary surface or exobase, causes chemical processes, heating effects and the possible ejection of atoms and molecules. Particle and radiation induced chemical surface processes are called space weathering. Space weathering is of considerable interest for the study of planetary bodies by remote sensing because it changes the optical surface properties (e.g., Hapke, 2001).

The first high quality broad-band spectrum of Mercury was obtained by McCord and Adams (1972). It seemed to be similar to the surface spectrum of the Moon, including an apparent pyroxene signature near 1 μm. This finding lead to the suggestion that the crust of Mercury was a high iron-titanium silicate like the lunar surface material in the maria. The low albedo and reddish slope of the spectrum is virtually identical to the Moon's, which strongly suggests a lunar type space weathering process on Mercury. These effects may be caused by submicroscopic metallic iron in the regolith, through deposition of vapors created by solar wind surface sputtering and vaporization by micrometeoroids (Hapke, 2001).

Killen et al. (2001) studied temporal and spatial variations in Mercury's Na exosphere and suggested that impact vaporization of micrometeoroids provides about 25% of the Na source with weak variations during a week. It was concluded that impact vaporization is an important but not the dominant source process for exospheric Na.

Space weathering effects on Mercury's regolith have been discussed in detail by Hapke (1977) and Rava and Hapke (1987). It is thought that Mercury's weak intrinsic planetary magnetic field can stand off the solar wind most of the time (Goldstein et al., 1981). However, magnetospheric models have shown that Mercury's magnetosphere could be open to the solar wind over substantial areas when the interplanetary magnetic field turns southward (Luhmann et al., 1998; Sarantos et al., 2001; Massetti et al., 2003). A strong magnetic field component B_x introduces a clear north–south asymmetry (Sarantos et al., 2001). Preferental precipitation is expected in the north when B_x is strongly negative, and in the south when B_x is strongly positive. The transition in enhanced Na emissions from south to north may correspond to the polarity of B_x.

Therefore, solar wind protons and heavier ions, can reach Mercury's surface where they will act as sputtering agents for the regolith. Lammer and Bauer (1997) showed that particle sputtering could be a source of hot N atoms with ejection speeds greater than 2 $\mathrm{km\,s^{-1}}$. Killen et al. (2001) concluded that increased ion sputtering resulting from ions entering through the cusp regions during favorable solar wind conditions is the probable mechanism leading to large and rapid increases in the Na content of Mercury's exosphere.

Yakshinskiy and Madey (1999) found in laboratory studies that Na atoms are released via PSD from surfaces that simulate lunar silicates. They found that bombardment of such surfaces with ultraviolet photons with wavelengths $\lambda <$ 300 nm at temperatures of about 250 K causes very efficient desorption of Na atoms. Killen et al. (2001) used data from the Solar EUV Monitor (SEM) instrument on board of the Solar and Heliospheric Observatory (SOHO) and studied the total Na content between November 13 and 20, 1997 and assumed that there was no ion sputtering on the most quiet day of their data set. For that day they modelled the particle release from Mercury's surface by using PSD and the impendence matching theory of Melosh for micrometeoroid impact vaporization. Thus, PSD could be an efficient surface particle release process.

In a recent study, Leblanc and Johnson (2003) used a 3D Monte Carlo model for the study of Mercury's Na distribution ejected from the surface by thermal desorption, PSD, micrometeoroid vaporization and solar wind sputtering. They found that the Na density distribution become nonuniform from day to night sides, from low to high latitudes and from morning to afternoon because of rapid depletion of Na atoms in the surfaces of grains mainly driven by thermal depletion. Further, the shape of the exosphere, as it would be seen from Earth, may change with respect to Mercury's heliocentric position.

It is the purpose of this work to present models that show the efficiency of surface source processes of Mercury's exosphere for PSD and particle sputtering, and compare this with micrometeoroid impact vaporization along Mercury's eccentric orbit around the Sun. We will show that the source rates and fluxes of particles which are released from Mercury's surface depend on Mercury's distance from the Sun, the configuration of the interaction between the interplanetary and planetary magnetic fields, the planetary latitude, between the day and nightside and local surface areas that are unprotected by the planetary magnetic field.

Our study will help to verify the planned in situ measurements of Mercury's highly variable particle environment by the proposed NPA-SERENA instrument package on board ESA's BepiColombo MPO spacecraft.

2. Photon stimulated desorption along Mercury's orbit

In order to investigate the photon stimulated desorption of Na atoms from the surface of Mercury, the variation of solar UV photons incident on the planetary surface over its orbit needs to be calculated. To achieve this, a radiative transfer model was adapted for the case of Mercury. The model was previously developed for Mars (Patel et al., 2002, 2003), and used for investigations of surface UV fluxes under any martian conditions. The atmospheric component was removed, and the geometric component describing the input solar UV was modified for Mercury's orbit around the Sun.

Yakshinskiy and Madey (1999) found that visible and near-UV photons with wavelengths larger than 300 nm and energy $h\nu$ smaller than 4 eV cause little or no detectable desorption of Na. For UV photons with $h\nu$ larger than 4 eV, Na desorption starts and becomes very efficient at UV wavelengths below wavelengths of 248 nm ($h\nu$ greater than 5 eV). Therefore, we used the solar UV photon flux below 248 nm of 1.4×10^{15} photons $\mathrm{cm^{-2}\,s^{-1}}$ (Killen et al., 2001) and scaled from the lunar value to the mean Mercury solar distance of 0.3871 AU.

The solar photon flux incident on Mercury's surface (ϕ_{ph}) at any time can be found from:

$$\phi_{\mathrm{ph}} = \frac{\mu}{r^2}\phi_{0.3871}, \tag{1}$$

where $\phi_{0.3871}$ is the photon flux at 0.3871 AU, μ is the cosine of the solar zenith angle and r is the relative Sun–Mercury distance with respect to 0.3871 AU. r can be found from:

$$r = \frac{1-e^2}{1+e\cos\omega}, \tag{2}$$

where e is the eccentricity of Mercury's orbit (0.20563) and ω is the true anomaly (angular position of Mercury within its orbit relative to perihelion). μ is found from:

$$\mu = \sin\Theta\sin\delta + \cos\Theta\cos\delta\cos\eta, \tag{3}$$

where Θ is the planetary latitude, δ is the solar declination, and η is the local hour angle. δ is found through:

$$\sin\delta = \sin\epsilon\sin\omega, \tag{4}$$

where ϵ is the obliquity of Mercury. The hour angle is determined by:

$$\eta = \frac{2\pi t}{P}, \tag{5}$$

where t is the time from local noon in seconds, and P is the Mercury day length in seconds. Due to the spin–orbit resonance of 3 : 2 for Mercury, additional complications are introduced into modelling the variation over time. The apparent motion of the Sun in the sky is not uniform over the year, with retrograde motion of the solar disk causing a distortion of the geographic solar irradiation over the orbit. For the purpose of this study, only situations at local noon are investigated, i.e., $t = 0$. Thus, any desorption spectra will only apply to positions on Mercury which are directly facing the Sun.

The solar UV photon flux can now be found at any latitude and any point in Mercury's orbit. The flux of Na desorption created by incoming solar UV photons can now be calculated through the following equation (Yakshinskiy and Madey, 1999):

$$\phi_{\mathrm{Na,PSD}} = \frac{1}{4}\phi_{\mathrm{ph}} Q f, \tag{6}$$

where Q is the photon stimulated desorption cross-section for Na of 1.4×10^{-21} cm^2 by Killen et al. (2001) and f is the composition of the regolith abundance for Na in Mercury's surface in the order of about 0.0033–0.0053 (Morgan and Shemansky, 1991; Killen et al., 2001) and the factor $\frac{1}{4}$ gives a surface averaged value.

The photon sputtering yield depends critically on the low energy cut-off of photons capable of ejecting Na, since the cross-sections for PSD release process of Na decreases dramatically for longer wavelengths. However, the number of available solar photons increases dramatically towards longer wavelengths in this range.

Knowing the UV photon flux ϕ_{ph} along with its relation to the Na photon stimulated desorption flux, the variation of the Na flux from the Sun-orientated point on Mercury's surface over its entire orbit can now be determined. This calculation was performed for a thin latitude strip from the north to the south pole, and calculated over the Hermean orbit for the latitude strip directly facing the Sun, shown in Fig. 1.

It is emphasized here that the values shown in Fig. 1 are not for the same latitude strip over the year. The plot shows only the Na flux along a latitude strip that is directly facing the Sun, and thus the longitudinal value of the strip changes geographically throughout the orbit. Thus these data should only be regarded for determining the Na flux from the Sun facing latitude strip.

One can see from Fig. 1 that the largest PSD fluxes of Na occur near equatorial latitudes at perihelion, where $\phi_{\mathrm{Na,PSD}}$ is about 4.5×10^6 $\mathrm{cm^{-2}\,s^{-1}}$. At aphelion the Na flux values at the equatorial regions are of the order of $\phi_{\mathrm{Na,PSD}} = 1.5 \times 10^6$ $\mathrm{cm^{-2}\,s^{-1}}$. The PSD fluxes at latitudes greater than 75 degrees are small, and therefore there should not be any noticeable PSD sources at Mercury's polar areas.

Our Na PSD fluxes at the equatorial regions at aphelion and perihelion are lower than the estimated Na PSD fluxes by McGrath et al. (1986) of about 2.0×10^7 $\mathrm{cm^{-2}\,s^{-1}}$ to 2.0×10^8 $\mathrm{cm^{-2}\,s^{-1}}$ but larger than the estimated average Na PSD flux value of about 2.0×10^5 $\mathrm{cm^{-2}\,s^{-1}}$ by Killen et al. (2001) and Killen and Ip (1999). It was also argued by Killen and Morgan (1993) that the fluxes estimated by McGrath et al. (1986) are overly optimistic since they were based on data for alkali halides. Morgan and Shemansky (1991) estimated a lower Na PSD flux of about $\phi_{\mathrm{Na,PSD}} = 3.8 \times 10^4\ \mathrm{cm^{-2}\,s^{-1}}$.

By using the new UV model described above and the laboratory data for PSD processes of Yakshinskiy and Madey (1999), our study minimizes former discrepancies in the estimation of PSD stimulated fluxes for Na by nearly *four orders* of magnitude and yield an average PSD flux for Na at Mercury's equatorial region of about $3.0 \times 10^6\ \mathrm{cm^{-2}\,s^{-1}}$. By estimating the PSD source rates R_{PSD} of Na atoms, which are released from Mercury's surface, one must consider the decrease of flux as function of latitude. We arrive at an R_{PSD} between periherm and apoherm of about $1.0 \times 10^{24}\ \mathrm{s^{-1}}$. Our model results are comparable with observations by Killen et al. (2001) who found $7.6 \times 10^{23}\ \mathrm{s^{-1}}$ for November 13 and $1.4 \times 10^{24}\ \mathrm{s^{-1}}$ for November 20, 1997.

Laboratory experiments by Madey et al. (1998) regarding the desorption of alkalis on oxide surfaces yield cross-sections for K atoms which vary between $1.4 \pm 0.6 \times 10^{-20}\ \mathrm{cm^2}$ and $1.9 \pm 0.8 \times 10^{-21}\ \mathrm{cm^2}$ for wavelengths between 247.5 nm (5.0 eV) and 365 nm (3.5 eV). Where the maximum cross-section in these experiments is about $1.8 \times 10^{-20}\ \mathrm{cm^2}$ at 253.7 nm (4.9 eV). By using these cross-section values and lunar regolith values of Morgan and Shemansky (1991) of about 0.00035 for K atoms one gets PSD fluxes between $5.0 \times 10^7\ \mathrm{cm^{-2}\,s^{-1}}$ to $3.0 \times 10^8\ \mathrm{cm^{-2}\,s^{-1}}$.

However, by using lunar regolith values the results are very large compared to previous estimates of about $5.0 \times 10^4\ \mathrm{cm^{-2}\,s^{-1}}$ (Potter and Morgan, 1986, 1988a, 1988b; Sprague, 1992; Flynn and Mendillo, 1995). The observation by Potter and Morgan (1997) give a Na/K ratio of about 200. Figure 2 shows the PSD fluxes in the order of about $10^4\ \mathrm{cm^{-2}\,s^{-1}}$ for K atoms corresponding to the observed Na/K fractionation along a latitude strip that is directly facing the Sun.

One should note that real regolith on Mercury's surface is different from the material studied by Madey et al. (1998), since it has been irradiated,the alkali binding could be altered, the porosity of the material is unknown and sticking could be an efficient process. These factors can cut down the cross-section by more than an order of magnitude. Further, the surface layer can be depleted in alkali (Hapke, 2001; Madey et al., 1998).

3. Exospheric particle supply by surface sputtering

From ground based observations Potter and Morgan (1985) discovered strong emission features in the spectrum of Mercury at the Fraunhofer Na D-lines, attributed to resonant scattering of Sunlight from Na vapor in the exosphere.

Sodium line profiles in Mercury's Na exosphere reveal that the exosphere is generally five hundred degrees hotter than the surface: 1200 K near the subsolar point to 750 K over the poles (Killen et al., 1999). This may be an indication of a hot source with partial thermal accommodation. The observation of an extended sodium tail implies that approximately 10% of the source atoms are ejected with a velocity above $2\ \mathrm{km\,s^{-1}}$ (Potter et al., 2002). These atoms may reflect the high velocity tail of a sputter distribution (Johnson et al., 2002) or the high velocity component of a hyper-velocity impact vapor source, represented by a *Maxwellian* distribution at about 5000 K.

In environments where energetic atomic or ionized particles impinge upon a planetary surface, emission of atoms or ions results via sputtering. Several studies in the past tried to estimate the particle flux and related sputter rates from Mercury's surface by estimating an area over Mercury's poles where it is believed that energetic solar wind protons can penetrate Mercury's surface and act as sputter agents (e.g., McGrath et al., 1986; Sieveka and Johnson, 1984; Cheng et al., 1987; Killen, 1989; Johnson, 1990; Ip, 1993; Lammer and Bauer, 1997; Killen et al., 2001).

Killen et al. (2001) used the model of Sarantos et al. (2001) for the calculation of the open magnetic field line area. Recently, Massetti et al. (2003) modelled the shape and the dimension of the open magnetic field line regions at Mercury's cusps, and the penetration of magnetosheath plasma through the exosphere of Mercury to its surface. In particular, Massetti et al. (2003) derived the incoming proton flux by taking into account the particle acceleration due to the magnetic merging between Mercury's field and the interplanetary magnetic field. For the calculation of sputtering rates we used in our study their evaluated particle fluxes and surface areas as a function of open magnetic field line patterns, according to different solar wind conditions. This new approach gives for the first time a better comparison of the planetary efficiency of sputtering and PSD source rates on Mercury.

The theory of sputtering of monoelemental polycrystalline, or amorphous targets has been worked out in detail by Sigmund (1969). Sputtering from an atmosphere is calculated in exact analogy to sputtering from a solid surface (e.g., Haff and Watson, 1979; Johnson, 1990, 1994; Lammer and Kolb, 2001).

An estimation of the flux of energized particles released from Mercury's surface requires the solution of the transport equation for the flow of moving atoms in the surface material due to the impact of energetic ions. The number of recoil particles that are set in motion by an incident particle is directly proportional to the nuclear elastic energy deposited so that the sputter yield has the following general form (Sigmund, 1969; Johnson, 1990):

$$Y(E_A, \cos\Theta_A) \approx E_D(E_A, \cos\Theta_A) S_{\mathrm{eff}}, \tag{7}$$

where $E_D(E_A, \cos\Theta_A)$ is the net elastic collision energy deposited per unit path length at the surface by an incident ion of energy E_A and direction of motion to the surface normal given by $\cos\Theta_A$, and S_{eff} is the sputter efficiency. $E_D(E_A, \cos\Theta_A)$ is proportional to the number density of

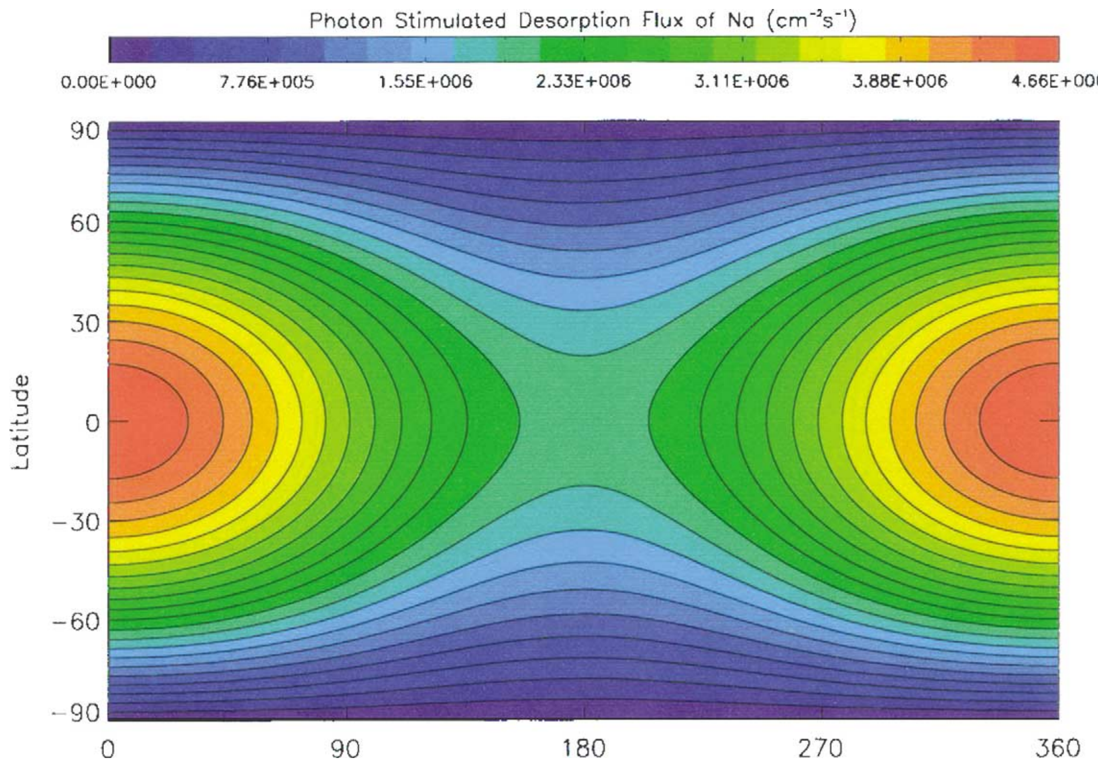

Fig. 1. Variation of the photon stimulated desorption flux of Na atoms as function of latitude from the Sun-orientated point on Mercury's surface over its entire orbit.

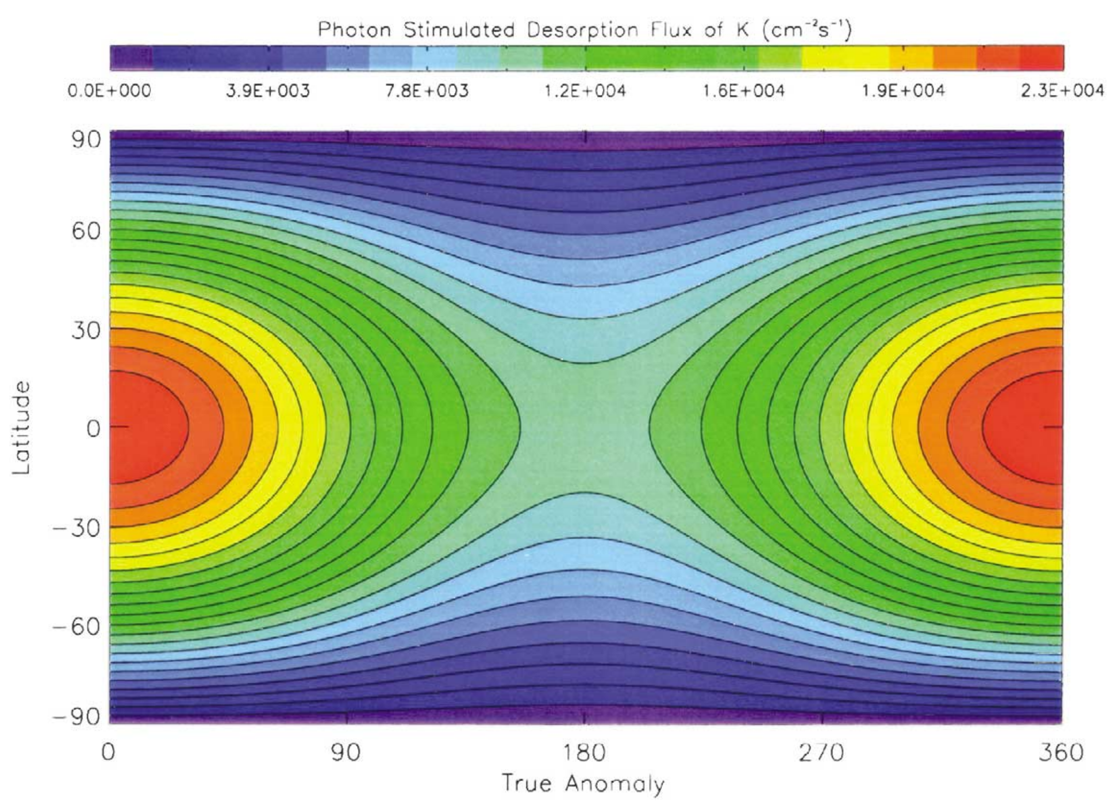

Fig. 2. Variation of the photon stimulated desorption flux of K atoms as function of latitude from the Sun-orientated point on Mercury's surface over its entire orbit.

the target atoms n_B (Sigmund, 1969):

$$E_D \approx \alpha \left(\frac{dE}{dx} \right)_n = \alpha n_B S_n, \tag{8}$$

where S_n is the nuclear elastic stopping cross-section of the incident ion and α is a collision parameter. Experimental values of α are taken from Fig. 3.17 of Johnson (1990). The sputter yield now has the following form (Johnson, 1990):

$$Y \approx \frac{3\alpha S_n}{2\pi^2 \sigma_d E_b} \approx \frac{0.042\alpha S_n}{E_b \,\text{Å}^2}, \tag{9}$$

where E_b is the binding energy of the atoms in the regolith particles and σ_d the average diffusion cross-section (Sigmund, 1969; Kelly, 1987; Cui et al., 1988). For the sputter ejection of many layers of a solid, E_b is roughly equivalent to the sublimation energy (Johnson, 1990). We use for our calculation of the stopping cross-section the *Universal Potential* of Ziegler et al. (1985). This potential and the corresponding stopping cross-section S_n fits well laboratory data for atomic collisions. It is close to the *Lenz–Jensen* potential but provides a better fit to experimental data and is used in most cases that describe average repulsive particle interaction processes (Johnson, 1990). The nuclear stopping cross-section is given by:

$$S_n = 2\pi \frac{A^2}{\gamma E_A} \big[2\varepsilon s_n(\varepsilon) \big], \tag{10}$$

where $s_n(\varepsilon)$ is the reduced stopping cross-section, E_A the energy of the incident particle, the ratio of incident m_A and sputtered m_B particle masses $\gamma = (4m_A m_B)/(m_A + m_B)^2$. A is obtained from the *Born Approximation* (Johnson, 1990):

$$A = \left(\frac{2m_A}{m_A + m_B} Z_A Z_B e^2 \right). \tag{11}$$

Z_A and Z_B are the nuclear charges of the incident and target particles, respectively. We use for our sputtering calculations the screening length a_u

$$a_u = \frac{0.8853 a_o}{(Z_A^{0.23} + Z_B^{0.23})}, \tag{12}$$

where a_o is the *Bohr* radius of an hydrogen atom and ε is the reduced energy:

$$\varepsilon = \frac{(\gamma E_A) a_u}{2A}. \tag{13}$$

The reduced stopping cross-section $s_n(\varepsilon)$ is for $\varepsilon > 30$ (Johnson, 1990):

$$\big[2\varepsilon s n_n(\varepsilon) \big] = \ln(\varepsilon), \tag{14}$$

and for $\epsilon < 30$

$$\big[2\varepsilon s_n(\varepsilon) \big] = \frac{\ln(1 + 1.138\varepsilon)}{1 + 0.0132\varepsilon^{-0.787} + 0.196\varepsilon^{0.5}}. \tag{15}$$

Figure 3 shows the stopping cross-section S_n for Na, O, Ca, and K atoms between the energy range of 500 eV up to 2 keV for protons. S_n is between 3.4×10^{-16} eV cm^2 and 5.6×10^{-16} eV cm^2 for Na atoms, between 3.15×10^{-16} eV cm^2 and 5.8×10^{-16} eV cm^2 for O atoms, between 1.9×10^{-16} eV cm^2 and 2.8×10^{-16} eV cm^2 for K atoms and between 1.8×10^{-16} eV cm^2 and 2.6×10^{-16} eV cm^2 for Ca atoms.

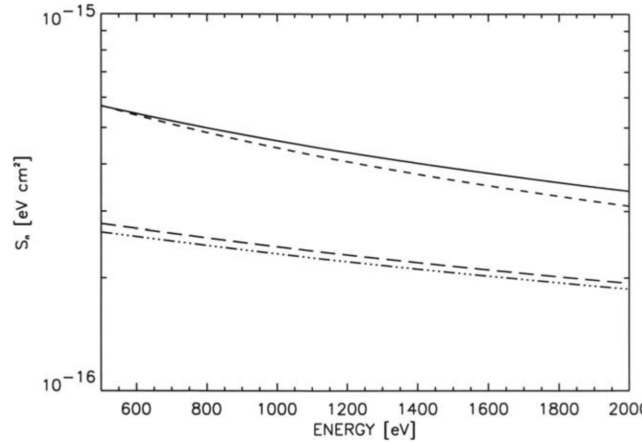

Fig. 3. Stoping cross-section S_n between protons and Na (solid line), O (dashed line), K (long-dashed line), and Ca (dashed-dotted-dotted line) atoms as function of energy.

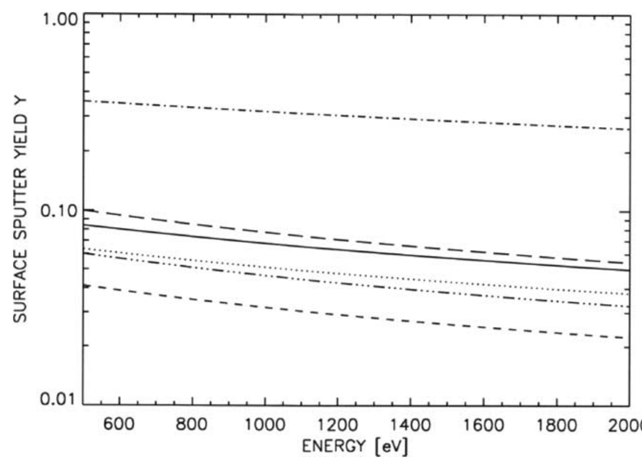

Fig. 4. Sputter yields for Na (dashed-dotted line, sputter agents Na^+, binding energy 2 eV; dotted line H^+ sputter agents, binding energy 2.65 eV; solid line H^+ sputter agents, binding energy 2 eV), O (dashed line), K (long-dashed line), and Ca (dashed-dotted-dotted line) atoms as function of energy and incident particles.

We used these stopping cross-sections for the calculation of the surface sputter yields. One can see from Fig. 4 that the sputter yield for O atoms is about 0.025–0.04, for K atoms about 0.054–0.1 for Ca atoms about 0.032–0.06 if solar wind protons are the incident particles. The yield for Na atoms is about 0.037–0.082 if solar wind protons are the incident particles and the Na binding energy is about 2–2.65 eV. The difference in the yield corresponds mainly to the different binding energies E_b between the species, which, depend both on the composition and chemical structure of the planetary surface.

Although Mercury's surface composition is not well known, Na is likely bound to O with a binding energy of about 2–2.65 eV, as for example in feldspar $NaAl_2Si_3O_8$ (McGrath et al., 1986; Cheng et al., 1987). In a recent study Leblanc and Johnson (2003) used a lower binding energy for Na of about 0.27 eV, which is based on laboratory experiments with pressed powder samples of Na_2SO_4 (Weins et al., 1997). This binding energy reduces the relative intensity of the high energy tail by at least one order of magnitude (Leblanc and Johnson, 2003). One can see from this discrepancies that measurements of Mercury's surface structure and composition are essential.

Since O atoms are also tightly bound to the molecule, the overall binding energy E_b is about 3–4 eV (Lammer and Bauer, 1997). The different binding energies reduce the sputter yield of O compared to Na atoms as long as more Na atoms are available in the bulk composition. For K atoms we use a binding energy of 2.4 eV (Wurz and Lammer, 2003).

Ca is also a good candidate for particle sputtering because of the large line-width found in optical observations (Bida et al., 2000) which is interpreted as a temperature of about 12000 K. Further, Ca was observed close to Mercury's polar areas (Bida et al., 2000; Killen and Morgan, 2000) where solar wind ions can penetrate to the planetary surface. We use a binding energy for Ca of 4 eV.

One can also see in Fig. 4 that the sputter yield for Na increases to about 0.27–0.35 if the incident particles are highly accelerated Na^+ ions, which may be accelerated back to the planetary surface (Ip, 1986). Na atoms can become ionized and consequently accelerated by the electric and magnetic fields of the magnetosphere (Ip, 1993). Some of these ions may also act as sputtering agents if their trajectories in the magnetosphere intersect the planetary surface. The flux of the sputtered particles $\phi_{sp,i}$ is

$$\phi_{sp,i} = f_i Y_i \phi_i \tag{16}$$

where f_i is the surface composition of constituent i, Y_i is the sputter yield of constituent i and ϕ_i is the precipitating flux of particles i. Massetti et al. (2003) calculated in our companion paper an average solar wind proton flux that can penetrate to Mercury's surface in the open magnetic field line area of approximately $4 \times 10^8\ cm^{-2}\,s^{-1}$.

We assume a Na composition for the regolith f_{Na} slightly enhanced over the lunar value of 0.0053 (Killen et al., 2001) and for O the lunar value of $f_O = 0.8$ (Morgan and Shemansky, 1991). Figure 5 shows the ejected particle fluxes $\phi_{sp,Na}$, $\phi_{sp,O}$, and $\phi_{sp,K}$ for Na, O, and K atoms if solar wind protons or backscattered Na^+ ions act as sputtering agents. By using the stopping cross-sections S_n and sputter yields calculated above (shown in Figs. 3 and 4) we arrive at proton induced sputter fluxes (shown in Fig. 5) for O of about 0.8–$1 \times 10^7\ cm^{-2}\,s^{-1}$, for Na of about 1.3–$1.6 \times 10^5\ cm^{-2}\,s^{-1}$ and about 1.0–$4.0 \times 10^4\ cm^{-2}\,s^{-1}$ for K atoms.

Using a magnetic field model Ip (1993) studied trajectories of Na^+ ions in Mercury's magnetosphere. It was found that low energy (< 3 keV) ions encounter the planetary surface at high latitude as a result of the finite size of the planet and the $\mathbf{E} \times \mathbf{B}$ drift pattern of the ions. High energy (> 10 keV) particles tend to hit Mercury's surface on the nightside hemisphere at low latitudes. By assuming an incident flux of backscattered Na^+ ions (Ip, 1993) of $1 \times 10^7\ cm^{-2}\,s^{-1}$ we obtain a sputtered Na flux of $2.5 \times 10^4\ cm^{-2}\,s^{-1}$.

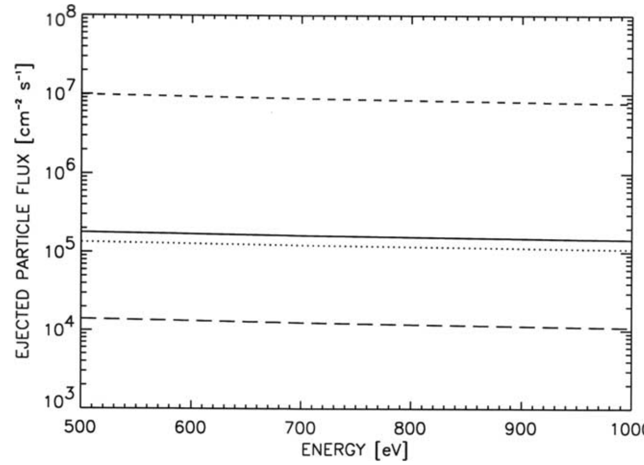

Fig. 5. Ejected particle fluxes for Na (dotted line, binding energy 2.65 eV; solid line, binding energy 2 eV), O (dashed line), and K (long-dashed line) atoms as function of energy and incident solar wind H^+ particles.

Although we do not currently know the exact flux values of precipitating magnetospheric heavy planetary ions on Mercury's surface, it seems that the sputter flux produced by this process is negligible compared to protons and particles which are released from Mercury's surface by PSD. However, future studies that model the Na^+ fluxes will clarify this problem if heavy ions may also enhance particle emissions in Mercury's exosphere.

From the model calculations of Massetti et al. (2003) we obtain an average estimated area where Mercury's surface is unprotected from its magnetic field and calculate the sputter rate for particles i

$$R_{sp,i} = \int_{A_s} \phi_{sp,i}\, dA, \tag{17}$$

from this area. A_s is an average area where the magnetic field lines are open. This area depends strongly on the magnetic field component B_z and the solar wind pressure P_{dyn}. However, Massetti et al. (2003) showed that it is possible to derive the open magnetic field line area where a value is about $2.8 \times 10^{16}\ cm^2$ if B_z is about minus 10 nT and P_{dyn} is about 20 nPa.

By taking this value for the open area and the mean average solar wind proton surface flux of about $4 \times 10^8\ cm^{-2}\,s^{-1}$ of Massetti et al. (2003) we derive an average Na sputter rate $R_{sp,Na}$ of about $4.2 \times 10^{21}\ s^{-1}$ and for O of about $2.5 \times 10^{23}\ s^{-1}$. The average sputter rate for K atoms is about $3.5 \times 10^{20}\ s^{-1}$, if we take lunar regolith values of about 0.00035 (Morgan and Shemansky, 1991). If one uses the lunar regolith values for Ca of about 0.062 (Morgan and Shemansky, 1991) we get a sputter rate of about $3.3 \times 10^{22}\ s^{-1}$.

By using the higher mean surface flux derived by the model of Massetti et al. (2003) of about 2×10^9 cm^{-2} s^{-1} of penetrating solar wind protons and the maximum area exposed to open magnetic field lines as estimated by Killen et al. (2001) of about 7.3×10^{16} cm^2, we deduce a total sputter rate for Na of about 5–6 $\times 10^{22}$ s^{-1}. For O atoms we get a sputter rate of about 3.5×10^{24} s^{-1} and for K about 5.0×10^{21} s^{-1}.

Killen et al. (2001) assumed a flux of precipitating solar wind particles onto Mercury's surface for the day on which they recorded the largest Na amount in the exosphere, solar wind particles with a density of about 120 cm^{-3} and a velocity of 3.22×10^7cm s^{-1} resulting in a flux of 3.9×10^9 cm^{-2} s^{-1}.

However, the estimations by Killen et al. (2001) were done by using a sputter yield that was twice as large as in this study, since they assumed that He and other heavy particles may also act as sputter agents. Further, they assumed that the area swept in the solar wind is about 4 times the area on the surface where the field lines intersect the surface.

One can see from this study that the results depend strongly on various parameters such as binding energies, solar wind density, magnetic field variability and Mercury's regolith composition. All of these parameters are not well determined at present due to the lack of experimental data, however, they influence the results depending on the input parameters chosen.

One should also consider that our calculated sputter yields are based on more or less ideal conditions. However, Johnson (1989) studied expressions for laboratory sputtering data in order to describe the effective yield from a planetary regolith composed of roughly spherical grains. It was found that for a fully exposed regolith the effective sputter yield is the order of 0.4 to 1 times the measured yield at normal incidence on a laboratory surface depending on the nature of the sputtering process. Further, it should also be noted that the laboratory sputter yield exhibit a dependence on incident angle (Johnson, 1989).

These experimental results indicate that our theoretically calculated sputter yields may correspond to upper limits and the real sputter yields on Mercury may be lower. Another effect, which should be studied in more detail in future work, is the efficiency of local trapping of sputtered particles due to the porosity of the soil, which is estimated to be 50 to 97% (Hapke, 1986; Johnson, 1989). Trapped atoms fractionated by differential desorption within the regolith is the most important process where chemical and optical alterations on planetary bodies, which are not protected by a dense atmosphere or a strong magnetic field, take place when the regolith is sputtered (Hapke, 2001).

Further, due to the energy dependence of the stopping cross-section the yield of sputtered particles can be reduced by a factor of 10 if accelerated high energetic protons with energies of about 10 keV to 30 keV act as sputter agents.

Our study shows that PSD of particles from Mercury's surface should be a more efficient process for Na compared to particle sputtering. Only during special solar wind conditions resulting in strong solar wind magnetosphere interactions can sputtering be comparable to the PSD process. One such event may have occurred between November 13 to 20, 1997, studied by Killen et al. (2001).

4. Impact vaporization by micrometeoroids

Impact vaporization of Mercury's regolith driven by hypervelocity meteoroid impacts were studied by Ip (1986), Morgan et al. (1988), Cintala (1992), and Killen et al. (2001). Meteoroid impact vaporization is the third most efficient particle source process in Mercury's exosphere. The source rates of Na, K, and other atoms added to Mercury's exosphere by impact driven processes depend upon the mass of material falling onto the planetary surface each second and the velocity distribution of the infalling material (Morgan et al., 1988; Divine, 1993; Mathews et al., 1997).

Meteorites have been considered both in the context of supplying Na and as a mechanism for water replenishment (Killen et al., 1997). Morgan et al. (1988) calculated the supply rate of Na from micrometeoroids to Mercury's exosphere by scaling the micrometeoritic mass flux at Earth of about 4.4×10^7 kg yr^{-1} to Mercury's orbit.

Their estimation showed that in the most extreme case where there is no Na assumed in Mercury's regolith micrometeoroids would supply the exosphere with a source rate R_{M} of about 1.5×10^{22} s^{-1}. If one assumes Na values in Mercury's surface material comparable to the amount which was found in lunar regolith then the supply rate can approach 1.4×10^{24} s^{-1} (Morgan et al., 1988). The latter value is comparable with source rates for Na caused by PSD and particle sputtering.

Eichhorn (1978a, 1978b) and Sugita et al. (1997) estimated in the laboratory from the emitted light from secondary particles produced during hypervelocity primary impacts the velocities and relative masses of the ejected particles as a function of the angle between the ejection direction and the target surface. The measured temperatures in the vapor cloud range between 2500 to 6000 K, depending on impact angles (Eichhorn, 1978a, 1978b; Sugita et al., 1997).

Given the density on the impact site one can assume *Maxwellian* like velocity distributions with mean velocity lower than 2 km s^{-1}. The results of these experiments show that micrometeoroid impact vaporization is a much more energetic process than PSD and can therefore also be responsible for the observations of Na D-lines also at higher altitudes.

A detailed study regarding the efficiency between both energetic particle release processes, surface sputtering and micrometeoroid vaporization will be possible through the proposed NPA-SERENA experiment, which will monitor Mercury on board of ESA's BepiColombo MPO spacecraft. This experiment consists of three different units, devoted to measure neutral particles from thermal energies up to tens of keV.

Hence, the exospheric particles composition will be analyzed by monitoring the local gas properties. At the same time, NPA-SERENA will be able to monitor the high energy part of the non-thermal (directional) neutrals, which will allow the investigation of the surface structure, as well as the related surface erosion processes.

5. Conclusions

By using a detailed UV model that gives the surface UV irradiance at any time and latitude over a Mercury year we found a solar UV *hotspot* is created towards perihelion, with significant average PSD particle fluxes and release rates. The average PSD induced Na fluxes are on the order of $3.0 \times 10^6\ \mathrm{cm}^{-2}\,\mathrm{s}^{-1}$ resulting in a Na source rate of about $1.0 \times 10^{24}\ \mathrm{s}^{-1}$, which may be comparable to rates released from Mercury's surface by micrometeoroid vaporization.

By using the laboratory obtained data of Yakshinskiy and Madey (2000) for the calculation of the PSD flux of K atoms we get fluxes up to about $3.0 \times 10^4\ \mathrm{cm}^{-2}\,\mathrm{s}^{-1}$. These flux values may be too high since they are based on idealized smooth surface conditions. PSD experiments on more realistic regolith analogue materials are needed in the future.

We used for the calculation of surface sputter fluxes the results of Massetti et al. (2003), obtained via a modified Tsyganenko T96 magnetosphere model. Using an average solar wind proton flux of about $4 \times 10^8\ \mathrm{cm}^{-2}\,\mathrm{s}^{-1}$ and an average estimated area of about $2.8 \times 10^{16}\ \mathrm{cm}^2$ where Mercury's surface is unprotected from the solar wind, we derive a sputter rate for Na of about $4.2 \times 10^{21}\ \mathrm{s}^{-1}$ and for O of about $2.5 \times 10^{23}\ \mathrm{s}^{-1}$.

The higher mean surface solar wind proton flux modelled by Massetti et al. (2003) of about $2 \times 10^9\ \mathrm{cm}^{-2}\,\mathrm{s}^{-1}$ of and the maximum area exposed to open magnetic field lines as estimated by Killen et al. (2001) of about $7.3 \times 10^{16}\ \mathrm{cm}^2$ yield a sputter rate for Na of about $6.0 \times 10^{22}\ \mathrm{s}^{-1}$. We estimate for this conditions a sputter rate for O atoms of about $3.5 \times 10^{24}\ \mathrm{s}^{-1}$ and for K atoms about $5.0 \times 10^{21}\ \mathrm{s}^{-1}$ by using lunar surface composition. The results depend strongly on various parameters such as surface binding energies, solar wind density and interplanetary magnetic field amplitude and direction, Mercury's regolith composition, as well as different lifetimes of the different released particles in Mercury's exosphere.

However, our particle sputtering rates correspond to precipitating solar wind protons which can act as sputter agents on the polar areas. One should also note that heavy ions which are accelerated in the magnetic field can also act as sputter agents if they hit Mercury's surface and may enhance the sputter rate.

Since particles released by PSD and surface sputtering have different source locations and energies the proposed NPA-SERENA instrument on board ESA's MPO will have the capability of separating all different particle source processes. The measurement of particles and effects that originate through micrometeoroid vaporization will yield a better understanding of the micrometeoroid exposure of planetary environments.

References

Bida, T.A., Killen, R.M., Morgan, T.H., 2000. Discovery of calcium in Mercury's atmosphere. Nature 404, 159–161.

Broadfoot, A.L., Shemansky, D.E., Kumar, S., 1976. Mariner 10: Mercury atmosphere. Geophys. Res. Lett. 3, 577–580.

Cheng, A.F., Johnson, R.E., Krimigis, S.M., Lanzerotti, L.J., 1987. Magnetosphere, exosphere and surface of Mercury. Icarus 7, 430–440.

Cintala, M.J., 1992. Impact induced thermal effects in the lunar and mercurian regoliths. Geophys. Res. Lett. 97, 207–208.

Cui, S.T., Johnson, R.E., Cummings, P.T., 1988. Molecular dynamics description of low energy cascades in solids: atomic ejection from solid Ar. Surf. Sci. 207, 186–206.

Divine, N., 1993. Five populations of interplanetary meteoroids. J. Geophys. Res. 98, 17029–17048.

Eichhorn, G., 1978a. Heating and vaporization during hypervelocity particle impact. Planet. Space Sci. 26, 463–467.

Eichhorn, G., 1978b. Primary velocity dependence of impact ejecta parameters. Planet. Space Sci. 26, 469–471.

Flynn, B., Mendillo, M., 1995. Simulations of the lunar sodium atmosphere. J. Geophys. Res. 100, 23271–23278.

Goldstein, B.E., Suess, S.T., Walker, R.J., 1981. Mercury: magnetospheric processes and the atmospheric supply and loss rates. J. Geophys. Res. 86, 5485–5499.

Haff, P.K., Watson, C.C., 1979. The erosion of planetary and satellite atmospheres by energetic atomic particles. J. Geophys. Res. 84, 8436–8442.

Hapke, B., 1977. Interpretations of optical observations of Mercury and the Moon. Phys. Earth Planet. Inter. 15, 264–274.

Hapke, B., 1986. On the sputter alteration of regoliths of outer Solar System bodies. Icarus 66, 270–279.

Hapke, B., 2001. Space weathering from Mercury to the asteroid belt. J. Geophys. Res. 106, 10039–10073.

Ip, W.-H., 1986. The sodium exosphere and magnetosphere of Mercury. Geophys. Res. Lett. 13, 423–426.

Ip, W.-H., 1993. On the surface sputtering effects of magnetospheric charged particles at Mercury. Astrophys. J. 418, 451–456.

Johnson, R.E., 1989. Application of laboratory data to the sputtering of a planetary regolith. Icarus 78, 206–210.

Johnson, R.E., 1990. Energetic Charged Particle Interactions with Atmospheres and Surfaces. Springer, Berlin, Heidelberg, New York.

Johnson, R.E., 1994. Plasma induced sputtering of an atmosphere. Space Sci. Rev. 69, 215–253.

Johnson, R.E., Leblanc, F., Yakshinskiy, B.V., Madey, T.E., 2002. Energy distributions for desorption of sodium and potassium from ice: the Na/K ratio at Europa. Icarus 156, 136–142.

Kelly, R., 1987. The sputtering of insulators. In: Mazzoldi, P., Arnold, G.W. (Eds.), Ion Beam Modifications of Surfaces. Elsevier, Amsterdam, pp. 57–113.

Killen, R.M., 1989. Crustal diffusion of gases out of Mercury and the Moon. Geophys. Res. Lett. 16, 171–174.

Killen, R.M., Ip, W.-H., 1999. The surface-bounded atmospheres of Mercury and the Moon. Rev. Geophys. 37, 361–406.

Killen, R.M., Morgan, T.H., 1993. Maintaining the Na atmosphere of Mercury. Icarus 101, 294–312.

Killen, R.M., Morgan, T.H., 2000. Discovery of calcium in Mercury's atmosphere. Nature 404, 159–161.

Killen, R.M., Potter, A.E., Morgan, T.H., 1990. Spatial distribution of sodium vapor in the atmosphere of Mercury. Icarus 85, 145–167.

Killen, R.M., Benkhoff, J., Morgan, T.H., 1997. Mercury's polar caps and the generation of an OH exosphere. Icarus 125, 195–211.

Killen, R.M., Potter, A.E., Fitzsimmons, A., Morgan, T.H., 1999. Sodium D_2 line profiles: clues to the temperature structure of Mercury's exosphere. Planet. Space Sci. 47, 1449–1458.

Killen, R.M., Potter, A.E., Reiff, P.H., Sarantos, M., Jackson, B.V., Hick, P., Giles, B., 2001. Evidence for space weather at Mercury. J. Geophys. Res. 106, 20509–20525.

Killen, R.M., Sarantos, M., Reiff, P.H., 2003. Evidence for space weather at Mercury. Adv. Space Res. In press.

Lammer, H., Bauer, S.J., 1997. Mercury's exosphere: origin of surface sputtering and implications. Planet. Space Sci. 45, 73–79.

Lammer, H., Kolb, C., 2001. Release processes of exospheric particles from Mercury's surface. Internal IWF Report. Space Research Institute Austrian Academy of Sciences, No. 136, 1–23.

Leblanc, F., Johnson, R.E., 2003. Mercury's sodium exosphere. Icarus 164, 261–281.

Luhmann, J.G., Russell, C.T., Tsyganenko, N.A., 1998. Disturbences in Mercury's magnetosphere: are the Mariner 10 substorms simply driven? J. Geophys. Res. 103, 9113–9119.

Madey, T.E., Yakshinskiy, B.V., Ageev, V.N., Johnson, R.E., 1998. Desorption of alkali atoms and ions from oxide surfaces: relevance to origins of Na and K in atmospheres of Mercury and the Moon. J. Geophys. Res. 103, 5873–5887.

Massetti, S., Orsini, S., Milillo, A., Mura, A., De Angelis, E., Lammer, H., Wurz, P., 2003. Mapping of the cusp plasma precipitation on the surface of Mercury. Icarus 166, 229–237.

Mathews, J.D., Meisel, D.D., Hunter, K.P., Getman, V.S., Zhou, Q., 1997. Very high resolution studies of micrometeors using the Arecibo 430 MHz radar. Icarus 126, 157–169.

McCord, T., Adams, J., 1972. Mercury: surface composition from the reflection spectrum. Science 178, 745–774.

McGrath, M.A., Johnson, R.E., Lanzerotti, L.J., 1986. Sputtering of sodium on the planet Mercury. Nature 323, 694–696.

Morgan, T.H., Shemansky, D.E., 1991. Limits to the lunar atmosphere. J. Geophys. Res. 96, 1351–1367.

Morgan, T.H., Zook, H.A., Potter, A.E., 1988. Impact-driven supply of sodium to the atmosphere of Mercury. Icarus 75, 156–170.

Patel, M.R., Zarnecki, J.C., Catling, D.C., 2002. Ultraviolet radiation on the surface of Mars and the Beagle 2 UV sensor. Planet. Space Sci. 50, 915–927.

Patel, M.R., Brces, A., Kolb, C., Lammer, H., Rettberg, P., Zarnecki, J.C., Selsis, F., 2003. Seasonal and diurnal variations in martian surface UV irradiation: biological and chemical implications for the martian regolith. Int. J. Astrobiol. 2 (1), 21–34.

Potter, A.E., Morgan, T.H., 1985. Discovery of sodium in the atmosphere of Mercury. Science 229, 651–653.

Potter, A.E., Morgan, T.H., 1986. Potassium in the atmosphere of Mercury. Icarus 67, 336–340.

Potter, A.E., Morgan, T.H., 1988a. Discovery of sodium and potassium vapor in the atmosphere of the Moon. Science 229, 651–653.

Potter, A.E., Morgan, T.H., 1988b. Extended sodium atmosphere of the Moon. Geophys. Res. Lett. 15, 1515–1518.

Potter, A.E., Morgan, T.H., 1990. Evidence for magnetospheric effects on the sodium atmosphere of Mercury. Science 248, 835–838.

Potter, A.E., Morgan, T.H., 1997. Evidence for suprathermal sodium atmosphere of Mercury. Adv. Space Res. 19, 1571–1576.

Potter, A.E., Killen, R.M., Morgan, T.H., 1999. Rapid changes in the sodium exosphere of Mercury. Planet. Space Sci. 47, 1441–1448.

Potter, A.E., Killen, R.M., Morgan, T.H., 2002. The sodium tail of Mercury. Meteorit. Planet. Sci. 37, 1165–1172.

Rava, B., Hapke, B., 1987. An analysis of the Mariner 10 color ratio map of Mercury. Icarus 71, 397–429.

Sarantos, M., Reiff, P.H., Hill, T.W., Killen, R.M., Urquart, A.L., 2001. A B_x interconnected magnetosphere model for Mercury. Planet. Space Sci. 49, 1629–1635.

Sieveka, E.M., Johnson, R.E., 1984. Ejection of atoms and molecules from Io by plasma-ion impact. Astrophys. J. 287, 418–426.

Sigmund, P., 1969. Theory of sputtering. I. Sputtering yield of amorphous and polycristalline targets. Phys. Rev. 184, 383–416.

Sprague, A.L., 1992. Mercury's atmospheric bright spots and potassium variations: a possible cause. J. Geophys. Res. 97, 18257–18264.

Sprague, A.L., Kozlowski, R.W., Hunten, D.M., Schneider, N.M., Domingue, D.L., Kells, W.K., Schmitt, W., Fink, U., 1997. Distribution and abundance of sodium in Mercury's atmosphere, 1985–1988. Icarus 129, 506–527.

Sprague, A.L., Schmitt, W.J., Hill, R.E., 1998. Mercury, sodium atmospheric enhancements, radar-bright spots, and visible surface features. Icarus 136, 60–68.

Stern, S.A., Fitzsimmons, A., Killen, R.M., Potter, A.E., 2000. A direct measurement of sodium temperature in the lunar exosphere. In: Proc. Lunar Planet. Sci. Conf. 31st, Houston, TX, p. 1122.

Sugita, S., Schultz, P.H., Adams, M.A., 1997. In situ temperature measurements of impact-induced vapor clouds with spectroscopic methods. In: Proc. Lunar Planet. Sci. Conf. 28th, pp. 1393–1394.

Weins, R.C., Burnett, D.S., Calaway, W.F., Hansen, C.S., Lykkem, K.R., Pellin, M.L., 1997. Sputtering products of sodium sulphate: implication for Io's surface and for sodium bearing molecules in the Io's torus. Icarus 128, 386–397.

Wurz, P., Lammer, H., 2003. Monte Carlo simulation of Mercury's exosphere. Icarus 164, 1–13.

Yakshinskiy, B.V., Madey, T.E., 1999. Photon-stimulated desorption as a substantial source of sodium in the lunar atmosphere. Nature 400, 642–644.

Yakshinskiy, B.V., Madey, T.E., 2000. Desorption induced by electronic transition of Na from SiO_2: relevance to tenous planetary atmospheres. Surf. Sci. 451, 160–165.

Ziegler, J.F., Biersack, J.P., Littmark, U., 1985. The Stopping and Range of Ions in Solids. Pergamon Press, New York.